Final Report

N70-20588

LIDAR OBSERVATIONS IN RELATION
TO THE ATMOSPHERIC WINDS ALOFT

By: W. VIEZEE   J. OBLANAS   R. M. ENDLICH

CASE FILE
COPY

Final Report

November 1969

LIDAR OBSERVATIONS IN RELATION TO THE ATMOSPHERIC WINDS ALOFT

By: W. VIEZEE   J. OBLANAS   R. M. ENDLICH

Prepared for:

AERO-ASTRODYNAMICS LABORATORY
AEROSPACE ENVIRONMENT DIVISION
ATMOSPHERIC DYNAMICS BRANCH
GEORGE C. MARSHALL SPACE FLIGHT CENTER
NATIONAL AERONAUTICS AND SPACE ADMINISTRATION
HUNTSVILLE, ALABAMA 35812

CONTRACT NAS 8-21117

SRI Project 7380

Approved:

R. T. H. COLLIS, *Director*
Aerophysics Laboratory

RAY L. LEADABRAND, *Executive Director*
Electronics and Radio Sciences Division

Copy No. 15

ABSTRACT

Lidar (laser radar) observations of the visually clear troposphere between 6 and 14 km are compared with data from simultaneous rawinsonde and Jimsphere ascents for the purpose of exploring possible relationships between lidar echoes and the atmospheric winds aloft. Because of its low intensity, the backscattered laser signal was monitored by means of a pulse-counting technique. The data indicate that the level of maximum wind speed corresponds to a level of relative increase in the optical density of the atmosphere as detected by the lidar. For the data examined, this level lies either at the tropopause or under the tropopause near layers of relative stability as shown by the temperature profile. The increase in optical density represents an increase in the concentration of particulate matter. Since its level corresponds to the average altitude for cirrus clouds, it is believed that the increase in particle density detected by the lidar is due to advection and/or formation of ice crystals near the level of maximum wind. It is concluded that the lidar-observed turbidity profile of the upper troposphere may be of value in inferring wind shear or layers of maximum wind speed, particularly in terms of extending information acquired by conventional means to other times.

CONTENTS

ILLUSTRATIONS

TABLES

I   INTRODUCTION

In connection with the launch of large space vehicles, there is a need for better measurement and prediction of wind conditions aloft. The best existing method of measuring upper winds has been the FPS-16 radar/Jimsphere technique, which additionally has possibilities for identifying turbulence.

The recent advent of the laser as a source of optical energy prompts consideration of optical ranging techniques for measuring and predicting upper winds. A number of approaches have been suggested, and some have been tried experimentally. In principle, lidars, or optical radars, could be used to measure upper winds in a variety of ways. The most obvious approach is to track ascending or falling targets--such as balloons or parachutes--in the same way as the FPS-16 currently does. Since the resolution and tracking capabilities of the FPS-16 radar are very good, there is little advantage in employing optical radars for balloon tracking. Some possibility exists, however, for tracking more tenuous targets--such as puffs or trails of chemical smoke introduced into the atmosphere by rockets. Although photogrammetric techniques have traditionally been used for such tracking, the range-determining capability of lidar might be a great advantage in this application. Another possibility is to make use of natural particulates in the atmosphere to study motion aloft. For example, where cirrus clouds or other particulate matter concentrations occur, wind motion could be derived by observing the displacement or the local changes of such features with time as they move in or with the wind field. Current lidar experience indicates a substantial possibility of making such observations under suitable conditions, using proposed equipment that is within the state of the art (Evans, 1968).[*] Apart from simple

---

[*]References are listed at the end of the report.

tracking, this approach offers considerable scope for more sophisticated techniques, such as have been considered and explored at radar frequencies.

The most powerful approach would be direct application of Doppler radar techniques to lidar systems that would be capable of analyzing the frequency shifts in backscattered energy, which are due to motion in the natural aerosol concentrations. Various forms of this concept have been studied, especially in connection with detecting clear-air turbulence using propagation of coherent laser light. The principal advantage of extending the Doppler technique to the optical spectral region is that, because of the very short wavelength of visible light much greater spatial resolution is possible than with microwave or radio systems. In addition, the absolute shift is much larger at optical frequencies, thus offering the possibility of improved precision in the velocity measurement (Owens, 1969). A laser Doppler velocimeter has been demonstrated in the laboratory for measurement of highly localized flow velocities in gases and liquids (Foreman et al., 1966). In the real atmosphere, however, velocity measurements with a ground-based laser are not yet feasible beyond distances of 40 to 70 meters and even within these distances artificial tracers are required (Owens, 1969).

At present, we feel that the most promising approach is to investigate the possibility of using lidar observations of energy backscattered by layers of particulate matter to supplement and extend (in space and time) data acquired by FPS-16/balloon soundings. On the premise that variations in the lidar-observed backscatter profile are associated with variations in the wind profile (i.e., shear layers), the capability of lidar to monitor continuously the backscattering properties of the atmosphere suggests that such observations could be used in extrapolating data acquired in previous FPS-16 soundings. Thus, more timely information on the height (and perhaps intensity) of wind shears can be obtained with a series of lidar/balloon ascents. This approach has been explored under the current contract. A limited sample of nighttime lidar observations of the upper troposphere (6 to 14 km) has been obtained in conjunction with FPS-16/Jimsphere and

2

GMD-1 rawinsonde ascents. The backscatter profiles from the lidar
suggest that concentrations of particulate matter are frequently present
under the tropopause near levels of high wind speed and large vertical
wind shear. The observations tend to substantiate the ultimate feasi-
bility of some of the suggested techniques for lidar measurements of
the atmospheric winds aloft.

II INSTRUMENTATION AND OBSERVATIONAL TECHNIQUE

Observations of the backscattering properties of a visually clear upper troposphere with a ground-based ruby lidar involve the detection of very-low-energy signals. In this case, quantitative measurements must be based on "pulse counting" rather than on "anode-current waveform" analysis.

The accepted technique for measuring low-energy signals is to employ a photomultiplier having a small cathode area (small source of thermally emitted electrons) and sufficient electron multiplier gain (10^7 or more) so that anode pulses resulting from individual photon absorption events at the photocathode can be viewed on an oscilloscope connected to the multiplier output (Morton, 1968). Each photon incident on the photocathode has a given probability (frequently called quantum efficiency) of causing the emission of a photoelectron. Each emitted electron triggers a cascade of approximately 10^7 electrons from the multiplier section of the phototube; this cascade appears as an individual anode-current pulse on the oscilloscope display. A count of these discrete anode-pulses per unit time interval is related to the arrival rate of photons at the photocathode. The arrival rate of photons, in turn, represents the atmospheric-backscatter signal. At large-energy signals, the rate of photons incident on the photocathode is high. Consequently, the pulse rate (the number of pulses per unit time) at the photomultiplier output becomes so great that the period between pulses becomes comparable to the pulse width; in this case, the pulses tend to overlap and can no longer be displayed and counted individually. Large signal levels are therefore, measured by reading the anode current resulting from the integration of many overlapping pulses. The pulse-counting technique has been successfully used in many investigations of the upper atmosphere by lidar (Bain and Sandford, 1966; Collis and Ligda, 1966; Nishikori et al., 1965).

4

Data collected under the contract were obtained with the SRI Mark V ruby lidar. The basic characteristics of the lidar's transmitter and receiver system are listed in Table I. The S-20 photocathode used by the multiplier has approximately a 2 percent quantum efficiency at the ruby wavelength.

Table I

CHARACTERISTICS OF MARK V LIDAR

Transmitter	
Laser Material	Ruby
Wavelength	6943 Å
Energy output per pulse	0.22 Joule
Pulse duration	15 nanoseconds
Peak power	15 megawatts
Aperture	6-inch Newtonian telescope
Beam divergence	3×10^{-4} radian
Cooling	Forced air
Q-switch	Rotating prism and saturable dye
Receiver	
Aperture	6-inch Newtonian telescope
Effective aperture area	0.01 m^2
Solid angle of view	Adjustable, 0.5 to 4.0×10^{-3} radian
Filter bandwidth (3-dB attenuation)	13 Å
Photomultiplier	RCA 7265 (S-20 cathode)
Display	Tektronix Model 555 dual beam CRO (bandwidth = 30 MHz) with P-11 Phosphor; Polaroid camera, Type 410 film; Logarithmic response video amplifier (optional)

The exact operating procedure used for obtaining the observations presented and discussed in this report was as follows. The lidar was pointed toward the zenith sky and lidar pulses were transmitted at a rate of one 15-ns pulse per minute. Each pulse represents approximately 0.22 Joule of energy. When the lidar is fired too rapidly, excessive temperature rise in the ruby crystal decreases the output energy and increases the ruby wavelength toward the water vapor absorption line at 6943.8 Å. At present, the temperature of the ruby rod cannot be completely controlled during an extended period of operation. Furthermore, the wavelength of the output pulse cannot be measured conveniently. In the present experiment, the total output energy was monitored and found to remain relatively constant from pulse to pulse when firing the lidar at a rate of 1 pulse per minute. A nearly constant output energy indicates no excessive temperature fluctuations and no drift in and out of the critical absorption line. At each lidar firing, the atmospheric backscatter signal was recorded in terms of the number of anode-current pulses per 5-μs time interval (750 m height interval). By firing ten times while increasing, at each firing, the time delay at which the 5-μs interval of data is displayed on the oscilloscope face, the troposphere between 6 and 14 km was sampled in successive 750-m height intervals (one interval per single shot) over a period of about 10 minutes.

Because photon flux is a statistical quantity and the photomultiplier response (quantum efficiency of the photocathode, focussing of electrons onto the first dynode, and multiplier gain) show statistical fluctuations, it is necessary to average data from successive observations and from extended height intervals in order to derive meaningful information on atmospheric structure. Consequently, lidar observations were made over time periods of several hours and data were averaged for successive "soundings."

Backscatter data were recorded in the form of Polaroid photographs of a dual-beam oscilloscope display from which the number of pulses were visually counted. Figure 1 shows examples of these photographs. The beam on the left-hand side of each photograph presents photomultiplier
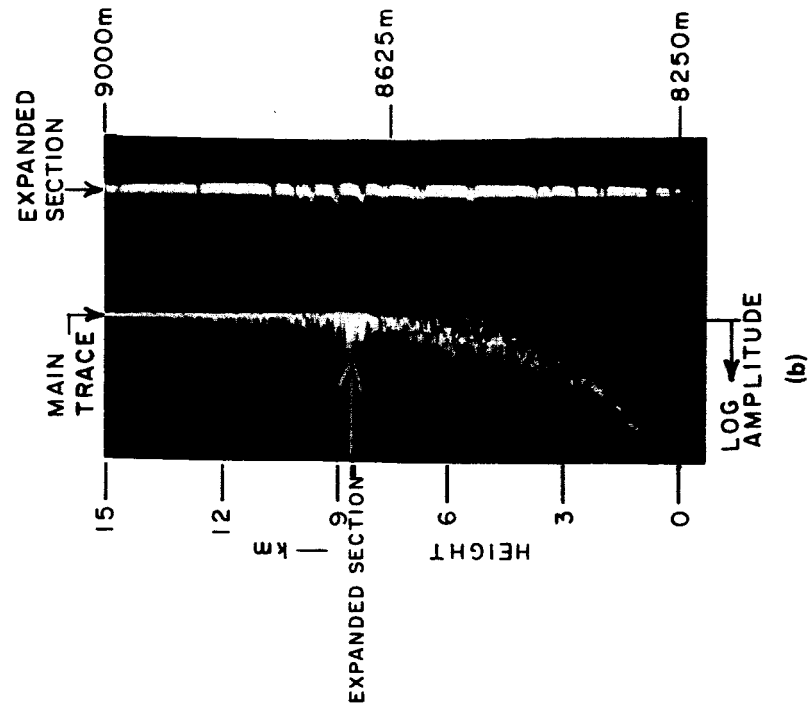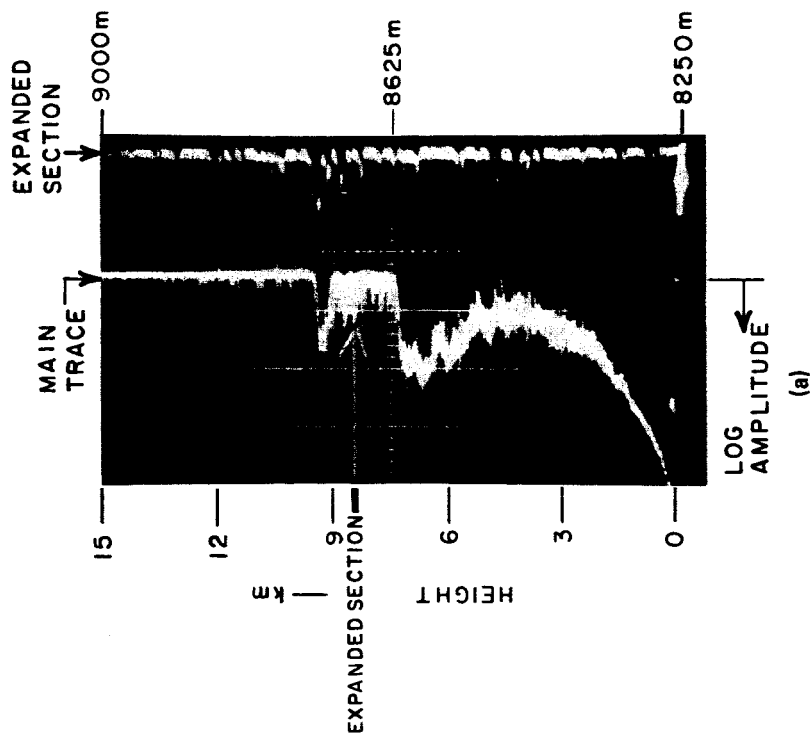
FIGURE 1 PHOTOGRAPHS OF DUAL-BEAM OSCILLOSCOPE DISPLAY USED TO RECORD LIDAR OBSERVATIONS. (a) 28 February 1969, 2118 PST (cloudy). (b) 4 March 1969, 2238 PST (clear).

anode current (obtained from pulse integration) on a logarithmic scale versus time on a linear scale (0 to 100 μs); this is equivalent to the logarithm of the receiver-output power versus range out to 15 km. This trace was used at each lidar firing to ascertain that no clouds were within the field of view. The trace on the right-hand side of the oscilloscope display shows (on a linear scale) the number of individual anode-current pulses recorded over a 5-μs time interval (750-meter height interval) of the left-hand side trace between 8250 and 9000 m. By properly time-delaying the oscilloscope sweep this expanded section can be triggered and displayed at any height along the main trace. The anode-current waveform shown in the left-hand side trace of Figure 1(a) is due to the large backscatter signal received from two cloud layers. The expanded 750-m height interval triggered between the cloud layers (right-hand trace) exhibits a high pulse count to the extent that pulses begin to overlap. In the absence of clouds, the backscattered radiation received from the same height interval is weak and consequently, the number of individual anode-current pulses can be readily determined by visual count as is evident from Figure 1(b). Another method of displaying the lidar data was also explored. From a multiple-trace oscilloscope display, eight separate, successive 750-m height intervals were photographed simultaneously at each lidar-pulse transmission. This technique, which was incorporated into the experiment by W. E. Evans,[*] was not sufficiently developed so that it could operate independently, owing to limitations of time and funding. It was used, however, to monitor the pulse count from 6 to 12 km on a shot-to-shot basis. Further development of this technique is recommended in future experiments.

During nighttime and under visually clear-sky conditions, the pulse-counting technique of data recording proved to be very effective between 6 and 14 km using the Mark V lidar system. Under these conditions, the measured sky background and the photomultiplier dark

---

[*]Senior Research Engineer, Electronics and Radio Sciences Division, Stanford Research Institute.

current noise are negligible with respect to the lidar backscatter signal from this tropospheric layer, which is in the range from 5 to 50 pulses per 5 μs. Below 6 km the recorded backscatter becomes relatively large (>70 pulses per 5 μs for our system) and frequent pulse overlap at the photomultiplier anode seriously affects the analyst's ability to count individual pulses accurately from the oscilloscope display. Above 14 km, the rate of photons incident on the receiver optics due to atmospheric backscatter is so low that fewer than 5 pulses per 5 μs are recorded by our system. In this case, the effects from sky background and internal system noise on the recorded data can no longer be ignored and data analysis becomes a laborious statistical process in order to separate signal from noise. It is essential that all observations be made in the absence of low and middle clouds. These clouds, which are nearly always water clouds, attenuate the transmitted lidar-pulse energy to the extent that no reliable backscatter data can be obtained from the atmospheric layers above. The absence or presence of clouds was determined by visual observations at the lidar site and by examining the logarithmic (left-hand side) trace in Figure 1 on a shot-to-shot basis.

Figure 2 shows an observed profile of pulse-count versus height obtained by averaging the counts from six consecutive soundings made during the evening of 3 March 1969. The profile is derived by assigning the average count for each 750-m height interval to the mid-level of the interval and connecting these values by straight lines. The indicated limits of the standard deviation are attributable to atmospheric varia-tions and to statistical fluctuations that are inherent in photon counting and in the overall system response. From shot to shot (level to level) the output energy of the lidar did not vary by more than 2 percent.

It is difficult to determine with precision from lidar observations the backscatter properties of the upper atmosphere in absolute terms. However, relative variations in backscatter from vertical layers, as revealed by the profile of Figure 2, are of considerable significance. Such relative variations can be determined to a high degree of confidence. To provide a general frame of reference for the lidar observations, the
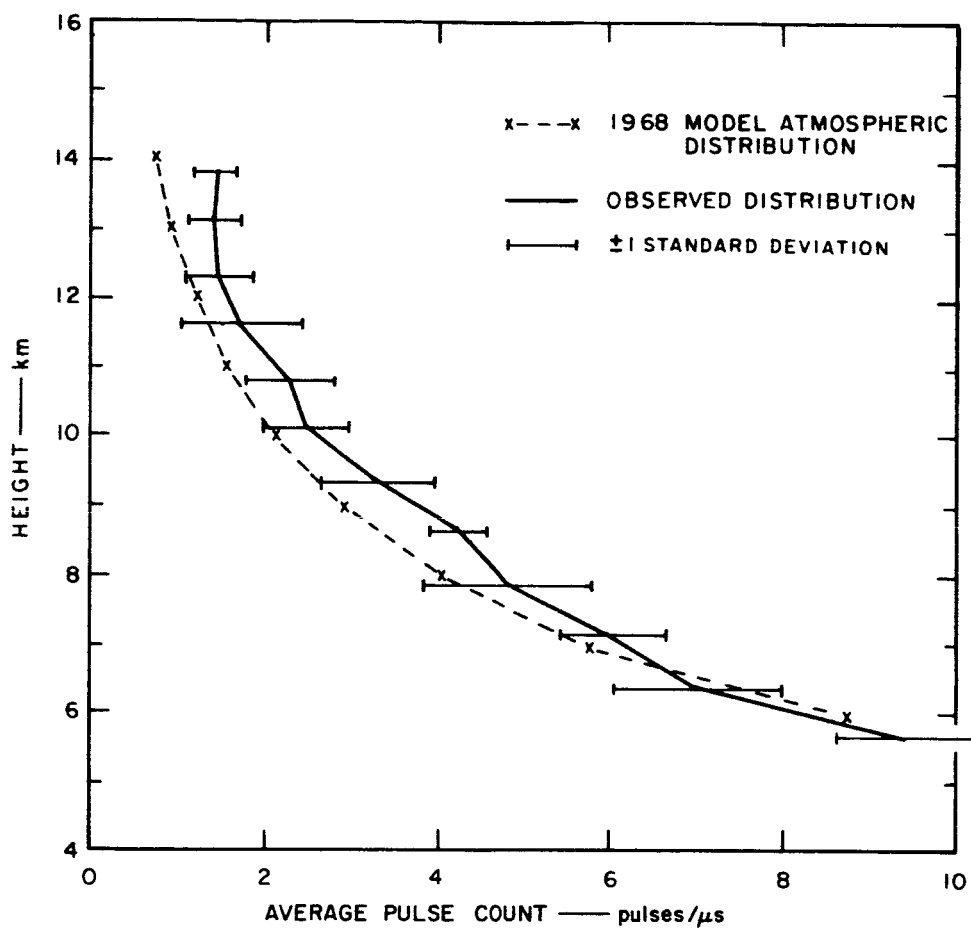
FIGURE 2   PROFILE OF PULSE COUNT AS A FUNCTION OF HEIGHT
OBSERVED BY LIDAR IN VISUALLY CLEAR UPPER
TROPOSPHERE (3 March 1969, 2011–2231 PST; predicted
Aerosol Model atmospheric distribution shown for comparison.)

Aerosol Model Atmosphere as tabulated by Elterman (1968) is used to approximate the photon density that could be expected at the receiver system of the Mark V ruby lidar after firing a single pulse in the following way. When a lidar pulse is transmitted through an atmosphere of which the scattering properties are precisely known, the number of photons backscattered from successive range intervals and incident per unit time on a narrow aperture of the receiver optics can be computed by means of the lidar equation. This equation, valid for single scattering only, can be written in the form:

$$P_r/A_r = \frac{P_t \tau c \beta_\pi e^{-2\bar{\sigma}R}}{2R^2} \qquad (1)$$

where

P_r/A_r = power incident on a unit area of the receiver aperture

τ = pulse duration

$P_t\tau$ = transmitted pulse energy

c = velocity of light

β_π = volume backscattering coefficient

$\bar{\sigma}$ = average extinction coefficient from lidar to target

R = one-way distance from lidar to target

For the ruby wavelength (approximately 6943 Å), one photon or quantum of energy equals 2.86×10^{-19} Joule. The average pulse energy, $P_t\tau$, of the Mark V lidar was found to equal approximately 0.22 Joule. Introducing these figures in Eq. (1) and substituting $c = 3 \times 10^2 \text{m} (\mu s)^{-1}$ gives

$$P_r/A_r = 1.16 \times 10^{20} \frac{\beta_\pi e^{-2\bar{\sigma}R}}{R^2}$$

photons per μs per unit area of effective receiver aperture.

11

Further computations can be carried out using the physical parameters of Elterman's 1968 Aerosol Model Atmosphere and the effective area of the receiver aperture for the Mark V ruby lidar. The average extinction coefficient, $\bar{\sigma}$, can be obtained directly from Elterman's tabulations. Assuming $\beta_\pi = 0.04\sigma_m$ (Bullrich, 1964) where σ_m = the aerosol attenuation coefficient listed by Elterman, and introducing $A_r = 0.01$ m^2 for the Mark V lidar, P_r (in photons per μs) can be computed between $R_1 = 6$ km and $R_2 = 14$ km. The resulting profile is shown in Figure 3. Table II shows the height variation of the ratio between the predicted values of Figure 3 and the lidar-measured pulse-count averaged for all lidar data collected during seven separate periods of observation. The ratios with respect to a Rayleigh (molecular) atmosphere have also been listed.

Table II

RATIO OF PREDICTED INCIDENT PHOTON RATE FOR AEROSOL AND RAYLEIGH
ATMOSPHERES TO MEASURED PULSE RATE FROM ACTUAL LIDAR OBSERVATIONS

HEIGHT (km)	Measured Pulse Rate (pulses per μs)	
	Predicted Photon Rate (photons per μs)	
	Aerosol Model Atmosphere	Rayleigh Atmosphere
6	1.0×10^{-3}	1.0×10^{-3}
7	1.2×10^{-3}	1.2×10^{-3}
8	1.2×10^{-3}	1.3×10^{-3}
9	1.4×10^{-3}	1.5×10^{-3}
10	1.3×10^{-3}	1.5×10^{-3}
11	1.4×10^{-3}	1.6×10^{-3}
12	1.5×10^{-3}	1.8×10^{-3}
13	1.5×10^{-3}	1.9×10^{-3}
14	1.7×10^{-3}	2.2×10^{-3}

It is interesting to note that the average ratio increases with height, which indicates that the atmospheric backscatter from the upper layers of the 6 to 14 km region does not decrease as rapidly with height as predicted on the basis of the Rayleigh atmosphere and the Aerosol Model Atmosphere. In order to illustrate this feature in the subsequent data
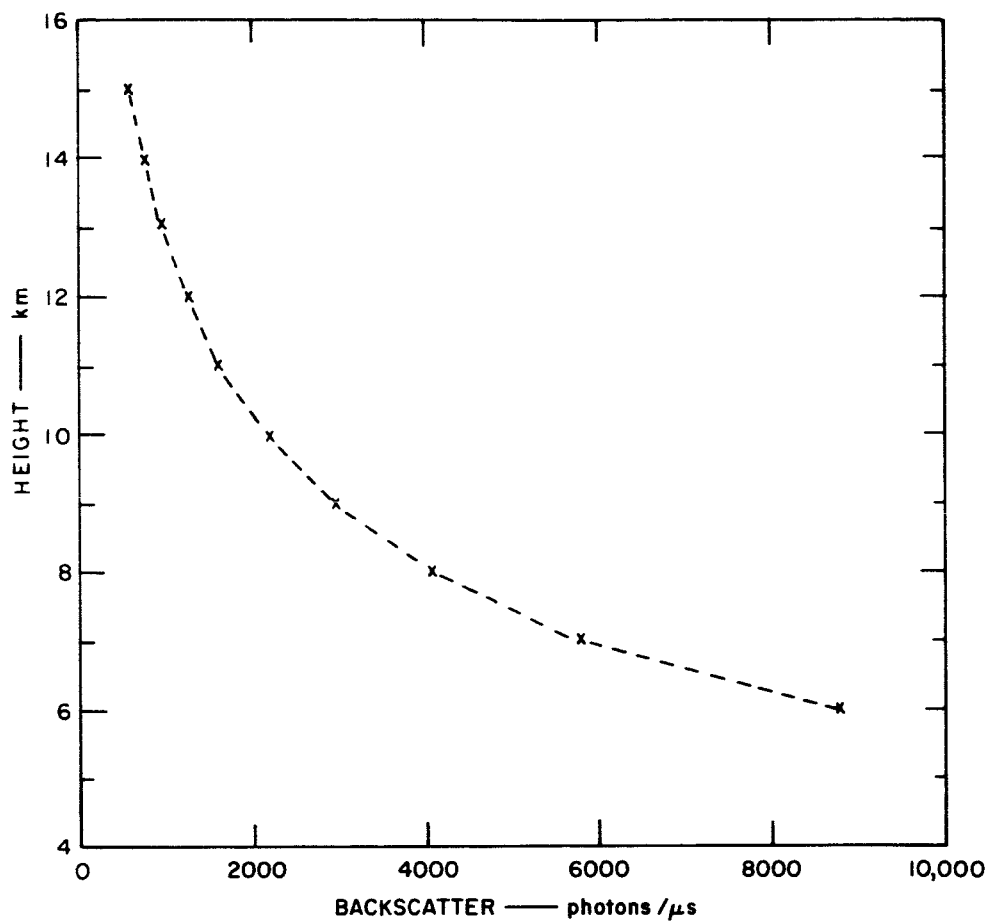
FIGURE 3   VERTICAL PROFILE OF BACKSCATTERED RADIATION INCIDENT
ON MARK V RECEIVER OPTICS AS COMPUTED
FOR 1968 AEROSOL MODEL ATMOSPHERE

analyses and at the same time to provide a common reference frame between the actual lidar measurements and those predicted on the basis of the Aerosol Model Atmosphere, the factor 10^{-3} is used to convert photons incident on the aperture of the telescope to pulses received at the photomultiplier output. This is equivalent to assigning arbitrarily an overall system efficiency or transfer of 10^{-3} to the Mark V lidar system. Thus, in Figure 2 and all subsequent similar figures, the dashed profile represents the backscatter from the 1968 Aerosol Model Atmosphere as recorded at the lidar receiver output in pulses per microsecond assuming a system efficiency of 0.1 percent.
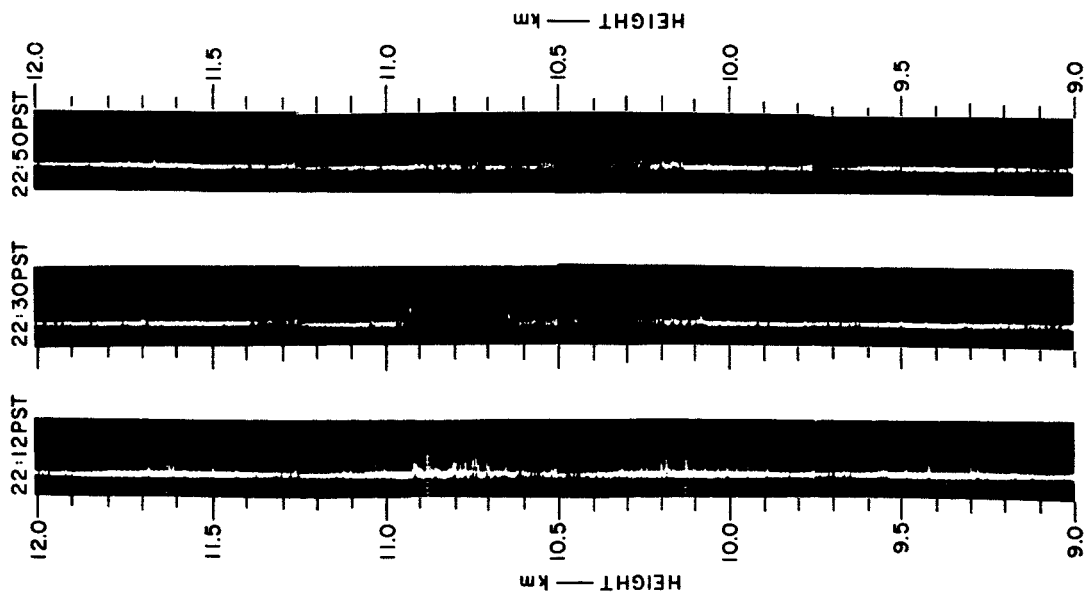
III DISCUSSION OF RESULTS

In this section, the lidar data and the comparative rawinsonde and Jimsphere data are presented and discussed within the framework of the contractual Statement of Work. Each one of the four tasks of the Work Statement is discussed separately.
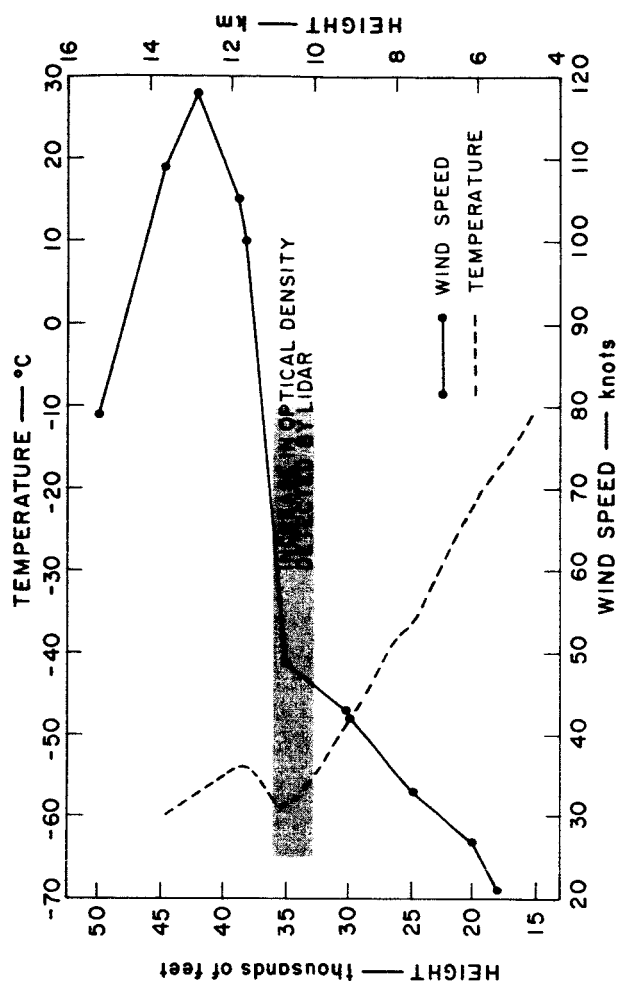
A. Task 1--Calibration of Equipment

> "...By operating the lidar at the SRI site, obtain
> a limited sample of data from heights near 10 km.
> The collection of these data will serve to prepare
> and calibrate the lidar equipment and associated
> data-recording facilities. This limited experiment
> also serves as a preparation for applying the basic
> technique of recognizing significant lidar returns
> from the upper troposphere to the field experiment
> of [Task 2]..."

Under Task 1, three nights of lidar observations were made at SRI in Menlo Park, California and the resulting pulse-count profiles compared with rawinsonde data from Oakland, California (about 20 miles away). The observations were made on 15, 16, and 28 January 1969.

On 15 January, data were collected primarily for the purpose of checking the proper operation of the lidar and the associated data-recording equipment and are not further discussed. On 16 January, between 2100 and 2300 PST, the lidar observed the presence of a tenuous layer of ice crystals at a height corresponding to that of the tropopause obtained in the Oakland rawinsonde ascent about four hours later. Figure 4(a) shows this feature as it appeared in the photographic data of the lidar soundings during three two-minute time periods, and Figure 4(b) shows the comparative rawinsonde data from Oakland. In Figure 4(a), the recorded pulse count is shown at each time in four consecutive height increments between 9 and 12 km. Within a period of about 40 minutes there were large variations in the recorded pulse rate between 10 km and 11 km. These represent variations in density of the

(b)   Wind and temperature profiles from rawinsonde ascent at Oakland, 17 January 1969, 0400 PST

(a)   Lidar profiles of pulse count as a function of height observed at Menlo Park, 16 January 1969, 2200-2300 PST

FIGURE 4   COMPARISON OF LIDAR AND RAWINSONDE DATA

16

particulate matter detected by the lidar. At 2230 PST, particle density increases to the extent that pulse pileup is sufficiently severe to prohibit a reliable count of individual quantitative pulses. Although the rawinsonde data from Oakland [Figure 4(b)] are not coincident in time, it is interesting to note that the layer in which concentrations of particulate matter are detected by the lidar lies immediately under the tropopause and also under a wind-speed maximum. Although no indications of cirrus cloud were apparent to observers at the lidar site, the official weather observation at Moffett Naval Air Station (10 miles southeast of Menlo Park) reported 2/10 to 3/10 thin cirrus; therefore, it may be assumed that the lidar detected rapidly varying concentrations of ice crystals.

Six consecutive lidar soundings were made between 2000 and 2300 PST on 28 January. Figure 5 shows the pulse count profile obtained by averaging the data from all six soundings for each 750-m height increment. Also indicated are the ±1 standard deviations of the measurements in each height group. Near 6 km the number of anode pulses normally becomes quite large and shows a tendency for overlap. Therefore, a large standard deviation at the start of the sounding can be partly attributed to errors made in distinguishing and counting individual pulses. At higher levels, i.e., above 8 km, a large standard deviation can arise from temporal variations in particulate-matter concentrations such as shown in Figure 4(a). The profile of pulse-count versus height predicted on the basis of the 1968 Model Atmosphere and the Mark V lidar parameters (Figure 3) is indicated in Figure 5 for comparison by assigning the assumed overall system efficiency of 0.1 percent. The bulge in the measured profile between 8 km and 10 km must be attributed to an increase in the concentration of particulate matter within the field of view of the lidar. Data from the Oakland rawinsonde ascents taken approximately four hours and twelve hours after the lidar observations suggest that the increase in lidar-measured pulse count may have been associated with a relatively stable layer in the temperature sounding starting just above 9 km and with a level of gradual wind-speed increase just below 9 km. The official record of surface observations
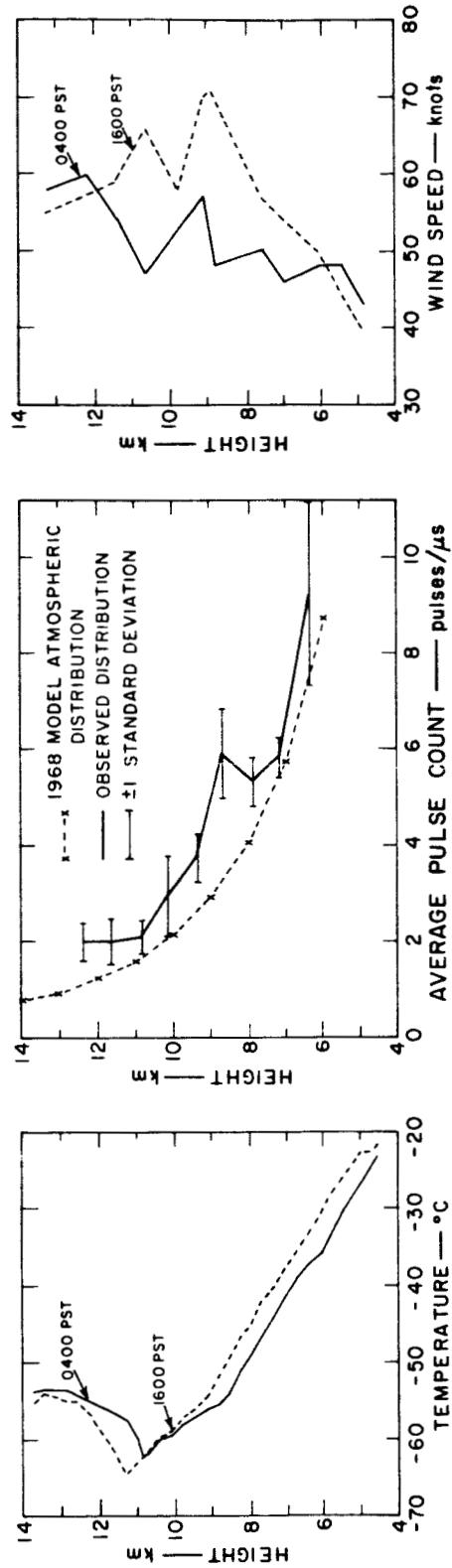
FIGURE 5   COMPARISON OF PROFILE OF PULSE COUNT AS A FUNCTION OF HEIGHT OBSERVED BY LIDAR AT MENLO PARK ON 28 JANUARY 1969, 2000–2300 PST, AND VERTICAL PROFILES OF TEMPERATURE AND WIND SPEED OBTAINED FROM RAWINSONDE ASCENTS AT OAKLAND, 29 JANUARY 1969

from Moffett Naval Air Station showed no reported middle or high clouds during the period of lidar operation.

B.   Task 2--Field Experiment

> "...Carry out a series of lidar observations of the
> clear atmosphere in conjunction with simultaneously
> measured Jimsphere wind profile data. Field measure-
> ments will be restricted to the Pt. Mugu site or
> the vicinity thereof..."

After work on the contract had been initiated, NASA and SRI agreed that the field measurement program could be more efficiently and conviently implemented by making lidar measurements at SRI in Menlo Park, while Jimspheres and radiosondes were released and tracked from Pillar Point, an AF/NASA radar missile-tracking facility 17 miles northwest of SRI. This arrangement enabled the SRI personnel and lidar equipment involved in the field experiment to remain in Menlo Park and to perform other duties in the absence of suitable weather conditions. Through the offices of the contract monitor and Mr. Charles Hines, NASA Vandenberg, arrangements were made to utilize a mobile GMD-1 unit from Vandenberg AFB to inflate and release Jimspheres and to make the necessary rawinsonde ascents at Pillar Point. Jimspheres were to be tracked with the AN/FPS-16 radar by personnel from Pillar Point. The change in physical setup of the field experiment proved to be fortunate, since adverse weather conditions during January and February caused frequent cancellation of planned nighttime experiments (recorded precipitation in Northern California during these two months was more than 200 percent of normal). Initially, observations were scheduled to begin during the week of 19 January 1969, but not one single cloud-free night occurred. Although weather conditions improved somewhat during the following week, we were informed on 27 January that, due to flooding near Vandenberg AFB, the rawinsonde and Jimsphere equipment could not be brought to Pillar Point until further notice. Subsequently, plans were made to conduct the experiment during the week of 10 February, but again heavy cloud cover, rain and the nonavailability of the AN/FPS-16

tracking radar at Pillar Point caused delay. Not until the night of
20 February were successful lidar/Jimsphere observations made. After
this date further unexpected delay was experienced. Finally, in con-
sultation with the project monitor, it was agreed that the week of
3 March 1969 would be the last week that the SRI lidar equipment could
be assigned to the project. During this week, however, four rawinsonde
and three Jimsphere ascents were obtained in conjunction with lidar
observations. These data, together with those obtained on 20 February,
constitute the observational results of the lidar/Jimsphere experiment.

C. Task 3--Analysis and Comparison with Jimsphere and Rawinsonde Data

> "...Analyze and compare the lidar measurements with
> Jimsphere profile measurements and available rawinsonde
> data..."

1. Comparison between Lidar and Rawinsonde Data

Figures 6, 7, and 8 show the lidar data and the comparative
rawinsonde data obtained during four observation periods. For each
period, lidar data are presented in the form of a vertical profile of
pulse count vs. height obtained by averaging the data from six to eight
consecutive soundings. Also indicated are the ±1 standard deviations
of the data for each height group.

Significant features in the lidar-measured profiles are
evaluated qualitatively on the basis of the indicated model atmospheric
profile and the standard deviations of the measurements. The layer in
which the measured count is judged to be relatively highest above model
atmospheric count is indicated by shaded blocks in both the lidar data
and corresponding rawinsonde data. This layer can be interpreted as
corresponding to a layer of increase in optical (particle) density. On
20 February [Figure 6] and on 7 March, 2201 - 2358 PST [Figure 8(b)],
the optical density increase coincides with a stable layer in the
temperature profile below the tropopause. On 5 March [Figure 7], it
lies below a sharp tropopause level, and on 7 March, 1903 - 2132 PST
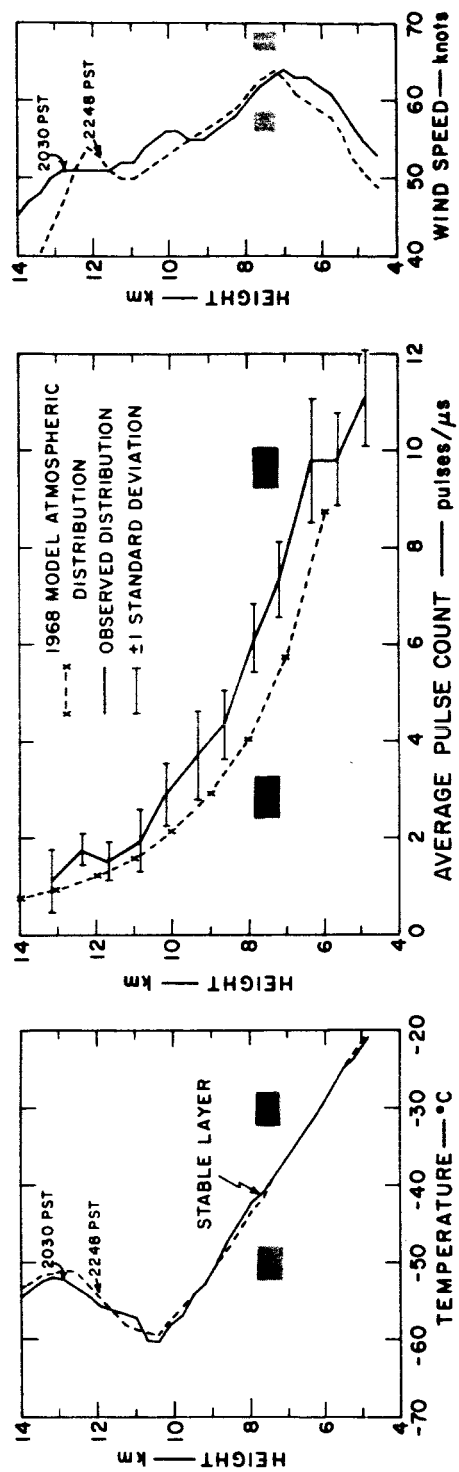[Figure 8(a)], below a tropopause layer. During all four observation

20

FIGURE 6   COMPARISON OF VERTICAL PROFILE OF PULSE COUNT OBSERVED BY LIDAR AT MENLO PARK ON 20 FEBRUARY 1969, 2000–2358 PST, AND VERTICAL PROFILES OF TEMPERATURE AND WIND SPEED FROM SIMULTANEOUS RAWINSONDE ASCENTS AT PILLAR POINT, 2030 AND 2248 PST
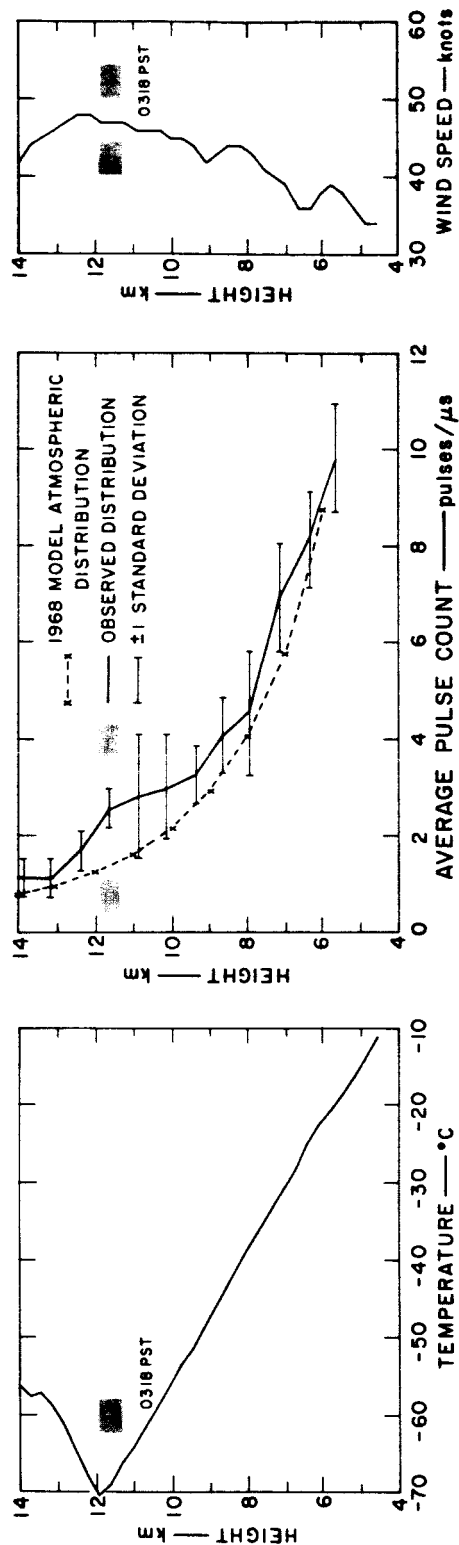
21

FIGURE 7   COMPARISON BETWEEN VERTICAL PROFILE OF PULSE COUNT OBSERVED BY LIDAR AT MENLO PARK ON 4/5 MARCH 1969, 2230—0312 PST, AND VERTICAL PROFILES OF TEMPERATURE AND WIND SPEED FROM RAWINSONDE ASCENT AT PILLAR POINT, 0318 PST
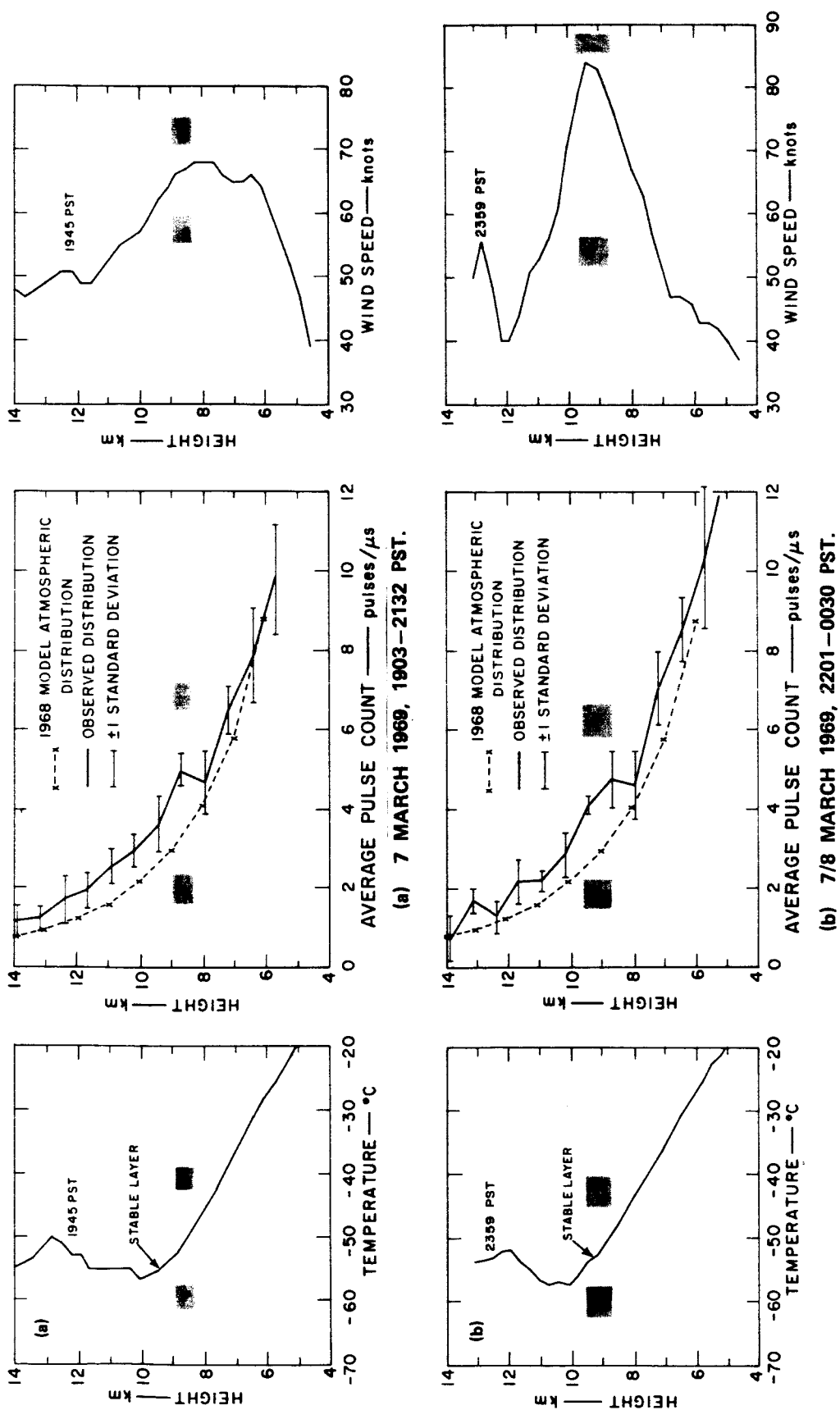
FIGURE 8   COMPARISON BETWEEN VERTICAL PROFILE OF PULSE COUNT OBSERVED BY LIDAR AT MENLO PARK
FOR NIGHT OF 7/8 MARCH 1969 AND VERTICAL PROFILES OF TEMPERATURE AND WIND SPEED
FROM SIMULTANEOUS RAWINSONDE ASCENTS AT PILLAR POINT.

23

periods, it is observed very close to the level of maximum wind speed. The observed lidar data of Figure 6 are not as convincing as those observed during the other periods. However, the layer of maximum wind speed is identified by a layer in which the lidar-measured pulse count is two standard deviations above the predicted count. The observations made during the night of 7 March 1969 are of particular interest, since they show that a large wind-speed increase took place in the layer where the optical-density increase was detected by the lidar. This feature is illustrated in more detail in Figure 9 by the vertical profiles of temperature change and wind speed change obtained from the data of the two rawinsonde ascents. During the observation period of four to five hours, a significant temperature increase (1° to 2°C) and wind speed increase (10-20 kts) is observed near the layer of large lidar-detected backscatter. A similar lidar backscatter/wind speed relation was suggested by the data of 28 January 1969 [Figure 5]. On 20 February [Figure 6], when two rawinsonde ascents were available also, no such wind speed increase occurred. The lidar, however, did not detect a pronounced increase in backscatter near the level of maximum wind speed and only on the basis of the standard deviation can a relative increase in the optical density be suggested. It is of interest to note that on 20 February and on 7 March a secondary wind speed maximum observed above 12 km is associated with a larger-than-average increase in lidar-detected optical density.

Examination of the official record of surface observations from Moffett Naval Air Station showed no middle or high clouds during the period of observation on 20 February and 7 March. On 4/5 March, however, very thin cirrus clouds were reported after midnight. It is, therefore, likely that the large increase in optical density detected by the lidar at the tropopause--and especially the large standard deviations involved in some of the measurements at lower levels--were the result of ice-crystal concentrations within the field of view of the lidar.
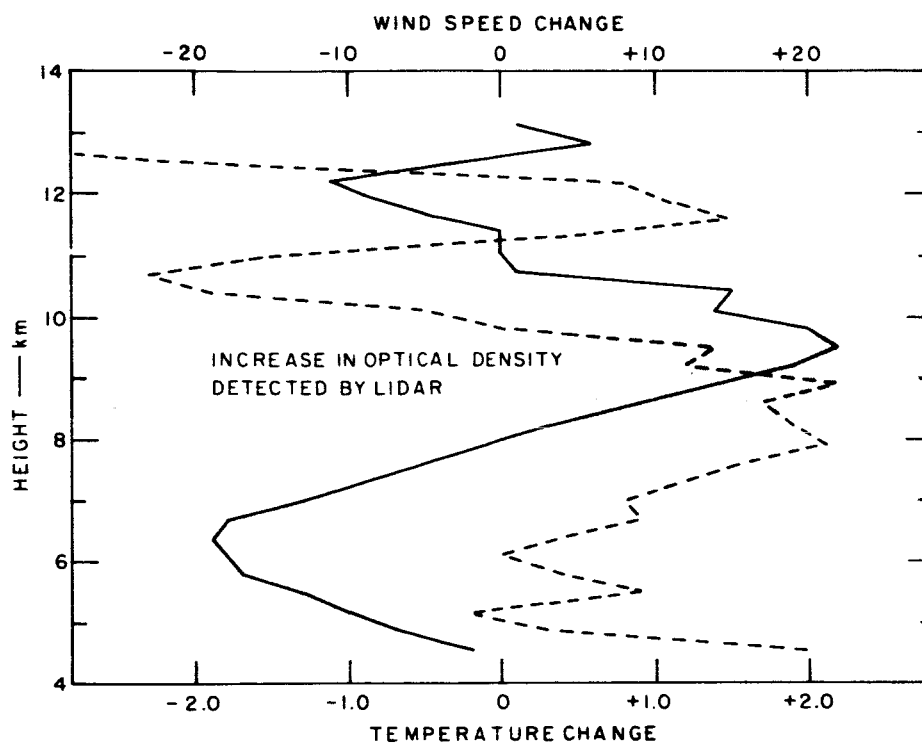
24

FIGURE 9   TEMPERATURE CHANGES (Dashed Profile) AND WIND-SPEED
            CHANGES (Solid Profile) OBSERVED BY SUCCESSIVE
            RAWINSONDE ASCENTS DURING LIDAR OBSERVATIONS
            ON 7 MARCH 1969

2.   Comparison between Lidar and Jimsphere Data

Lidar observations and simultaneous measurements of the vertical wind profile by Jimsphere are compared for two separate days. On 20 February 1969, two successive Jimsphere ascents were made at Pillar Point between 2000 and 2300 PST. The vertical profiles of the scalar wind speed obtained from these ascents are shown in Figure 10, together with the vertical profile of atmospheric backscatter as detected by the lidar. The latter is an average profile based on data from eight measurements made at Menlo Park, California between 2000 and 2400 PST. No pronounced increase in the observed optical density is evident, but average values of pulse rate near the level of maximum wind (7 to 8 km) are more than two standard deviations above the reference count of the Aerosol Model Atmosphere. The lidar data in this case, however, are ambiguous. The relatively small increase in pulse count observed between 12 and 13 km corresponds to a secondary wind speed maximum.

On the night of 7 March 1969, three Jimsphere ascents were made at Pillar Point. However, due to difficulties in data recording and processing, only one ascent is available for comparison. The lidar data on atmospheric backscatter collected between approximately 2200 and 2400 PST can be compared with data from the Jimsphere ascent made at 2356 PST. Figure 11 shows the data comparison. The lidar detected a pronounced increase in the optical density of the atmosphere between 8 and 10 km, which is the layer of maximum wind speed (44 m/sec). No significant variations in wind direction or in the vertical rise rate of the spherical balloon are evident in this layer. A secondary, higher-level increase in backscatter near 13 km does not correspond to a secondary wind-speed maximum in the Jimsphere data as on 20 February [Figure 10]. It is interesting to note, however, that the rawinsonde ascent did indicate a relative wind-speed maximum near this level [see Figure 8(b)].
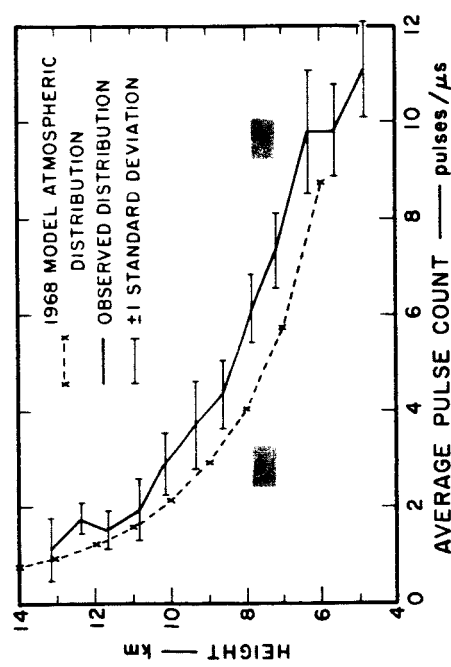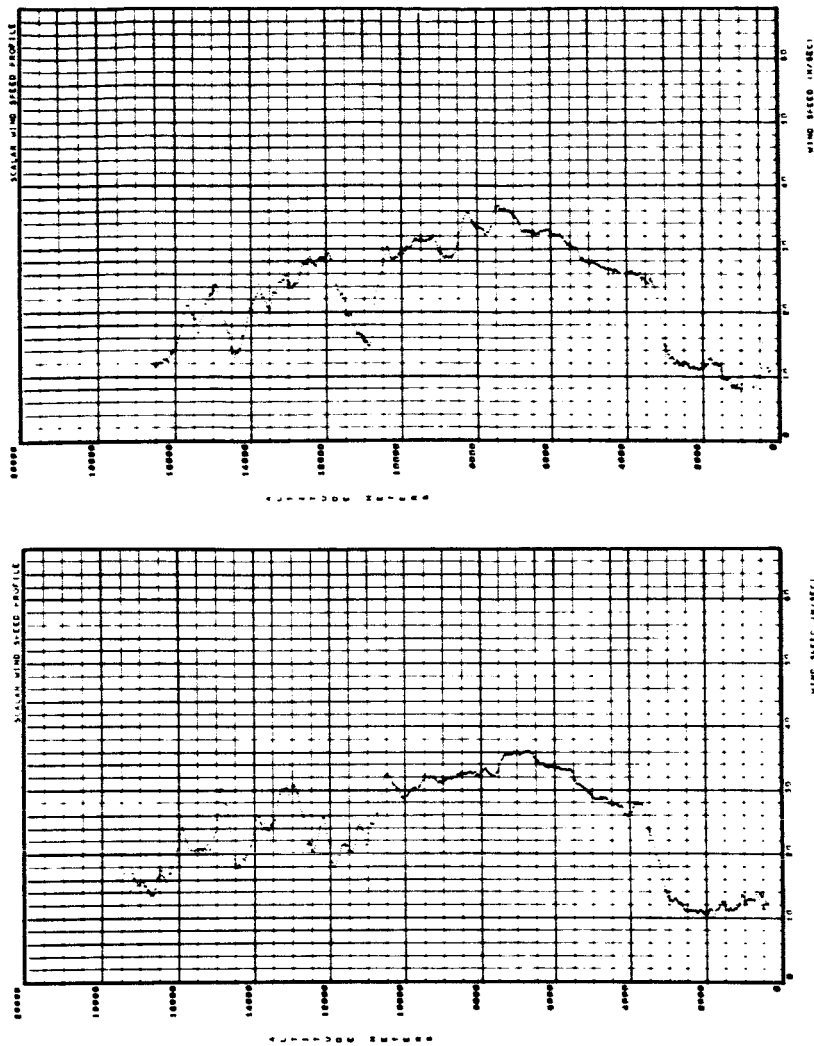
FIGURE 10 COMPARISON BETWEEN VERTICAL PROFILE OF PULSE COUNT OBSERVED BY LIDAR AT MENLO PARK ON 20 FEBRUARY 1969, 2000–2300 PST, AND VERTICAL PROFILES OF WIND SPEED OBSERVED BY TWO SUCCESSIVE JIMSPHERE ASCENTS AT PILLAR POINT (2008 PST and 2240 PST)
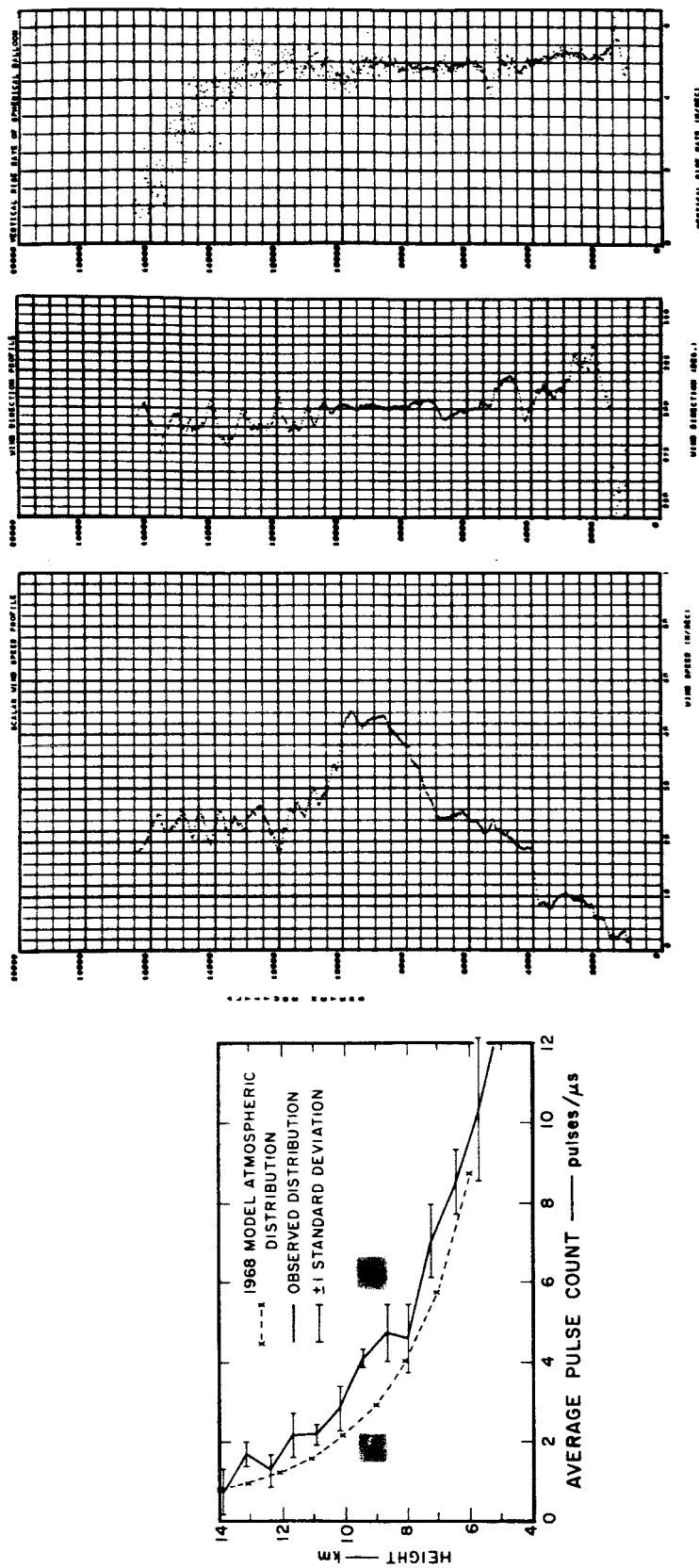
27

FIGURE 11 COMPARISON BETWEEN VERTICAL PROFILE OF PULSE COUNT OBSERVED BY LIDAR AT MENLO PARK ON 7 MARCH 1969, 2201–0030 PST, AND DATA FROM JIMSPHERE ASCENT AT 2356 PST AT PILLAR POINT

D. Task 4--Evaluation of Present and Potential Capabilities

> "...Evaluate the potential and/or existing capability
> of lidar for atmospheric wind measurements on the
> basis of the data comparison made under [Task 2]..."

On the basis of the limited data sample collected under the program, the following points of interest can be summarized:

(1) The lidar data suggest that the optical (particle) density of the atmosphere between 6 and 14 km does not decrease as rapidly with height, as predicted on the basis of the 1968 Aerosol Model Atmosphere.

(2) When lidar observations were made in conjunction with rawinsonde and Jimsphere ascents, the layer of maximum wind speed was identified in the lidar data as a layer of relatively high optical (particle) density.

(3) Temperature data from the rawinsonde ascents suggest that the lidar-detected layer of relatively large backscatter is associated with a stable thermal structure but not necessarily with the tropopause.

(4) The lidar-detected layer of large backscatter (8 km) has a relationship to the layer of maximum wind speed that is similar to that connected with cirrus clouds (James, 1957). Therefore, the layer of increase in optical density observed by the lidar during visually clear-sky conditions is believed to be associated with a haze layer or a layer of subvisible ice crystals which is advected and/or formed in the layer of maximum wind.

The limited observation program suggests that lidar can provide indirect information on the atmospheric winds aloft. From the results of the experiment it appears that the altitude of the layer of maximum wind speed can be identified. Also, a qualitative assessment of maximum

29

wind speed can possibly be made on the basis of the degree of increase in optical density detected by the lidar. However, a further evaluation of the capability of lidar to supply additional information on vertical wind shear and turbulence must await the accumulation of larger samples of data. These must be collected when low and middle clouds are absent, in order to avoid extinction of the laser pulse.

The technique of collecting lidar data used in the present study can be improved to the extent that all data between 6 and 14 km can be collected and displayed upon the transmissions of a single pulse. This would decrease the time interval between data readings for each sampled layer by a factor of 10. Furthermore, in subsequent experiments, the contribution to the standard deviation of the measurements from fluctuations in the system response should be more precisely determined. After this contribution is eliminated, the standard deviations can be entirely attributed to fluctuations in atmospheric optical density and should be compared to variations in the vertical wind shear and to the perturbations that have been observed in the ascent rates of Jimsphere balloons (Wheeler, 1969). For this purpose, lidar observations should be made in conjunction with temperature and wind soundings on a smaller scale than was done under the present program. For example, an experimental program involving the operation of a lidar within a mesoscale network of Jimsphere ascents would enable an assessment of the significance of a lidar-detected anomaly in both space and time.

ACKNOWLEDGMENTS

REFERENCES

Bain, W. C. and M. C. W. Sandford (1966), "Light Scatter from a Laser
Beam at Heights above 40 km." J. Atmos. Terr. Phys., Vol. 28,
pp. 543-552.

Bullrich, K. (1964), "Scattered Radiation in the Atmosphere and the
Natural Aerosol," Advances in Geophysics, Vol. 10, p. 99.

Collis, R. T. H. and M. G. H. Ligda (1966), "Note on Lidar Observations
of Particulate Matter in the Stratosphere," J. of Atmos. Sci.,
Vol. 23, pp. 255-257.

Elterman, L. (1968), "UV, Visible, and IR Attenuation for Altitudes to
50 km," Environmental Research Papers, No. 285, Air Force Cambridge
Research Laboratories, L. G. Hanscom Field, Bedford, Massachusetts.

Evans, William E. (1968), "Remote Probing of High Cloud Cover via
Satellite-Borne Lidar," Final Report Contract NAS-49(27), National
Aeronautics and Space Administration, Washington, D.C. 20546.

Foreman, J. W. Jr., et al. (1966), "Fluid Flow Measurements with a
Laser Doppler Velocimeter," IEEE J. Quantum Electronics, Vol. QE-2,
pp. 260-266.

James, D. G. (1957), "Investigations Relating to Cirrus Cloud,"
Meteorological Magazine, Vol. 86, No. 1, p. 015.

Midwest Research Institute (1968), "Study of Atmospheric and AAP
Objectives of Cross-Beam Experiments," Final Report Contract No.
NAS8-21065, National Aeronautics and Space Administration, George
C. Marshall Space Flight Center, Huntsville, Alabama 35812.

Morton, G. A. (1968), "Photon Counting," Appl. Opt., Vol. 7, No. 1

Nishikori, Kiyoshi, et al. (1965), "On Observations of the Upper Atmo-
sphere by Ruby Laser," J. Radio Res. Labs., Vol. 12, No. 62, pp. 213-22.

Owens, James C. (1969), "Optical Doppler Measurements of Microscale
Wind Velocity," Proc. IEEE., Vol. 57, No. 4, pp. 530-536.

Wheeler, R. S. (1969), "An Analysis of the Jimsphere Ascent Rate with a
Discussion of Vertical Motions in the Winds Aloft," NASA Contractor
Report, NASA CR-61276, Contract NAS8-5608, prepared by the
Boeing Company.